Interaction of Dicarboxylic Metalloporphyrins with Liposomes. The Effect of pH on Membrane Binding Revisited

Author(s): Mariusz Kępczyński and Benjamin Ehrenberg
Source: Photochemistry and Photobiology, 76(5):486-492.
Published By: American Society for Photobiology
DOI: http://dx.doi.org/10.1562/0031-8655(2002)076<0486:IODMWL>2.0.CO;2
URL: http://www.bioone.org/doi/full/10.1562/0031-8655%282002%29076%3C0486%3AIODMWL%3E2.0.CO%3B2

Photochemistry and Photobiology, 2002, 76(5): 486–492

Interaction of Dicarboxylic Metalloporphyrins with Liposomes. The Effect of pH on Membrane Binding Revisited¶

Mariusz Kępczyński† and Benjamin Ehrenberg*‡

Department of Physics, Bar Ilan University, Ramat Gan, Israel

Received 5 July 2002; accepted 20 August 2002

ABSTRACT

The acid–base properties of Zn-hematoporphyrin IX (ZnHP) and Zn-mesoporphyrin IX (ZnMP) and the effect of pH on their binding to liposomes have been studied. The ionization constants for the two carboxylate groups of ZnHP were calculated by principal component analysis and are 5.7 ± 0.1 and 6.9 ± 0.05. The neutral species and the mono- and di-anionic forms all bind to liposomes, but a strong pH effect on the binding constant was observed for both the investigated compounds. We also observed a decrease in the binding of the two anionic species when the membranes carried a negative charge. These results indicate that the porphyrins partition into the membrane with their carboxylic moieties near the lipid–water interface so that their deprotonation, leading to a charged molecule, does not prevent the insertion of the tetrapyrrole ring into the lipid environment of neutral liposomes.

INTRODUCTION

The acid–base properties of porphyrins with peripheral carboxylic acid groups have been the topic of several publications (1–10). The free-base form of such porphyrins contains two pyrrole nitrogens that are capable of gaining protons and two propionic acid residues that can dissociate. These sites allow the molecule to exist as different ionic species with different overall charge, depending on the pH of the environment. Savitski *et al.* (2) and Barrett *et al.* (5) discussed the theoretically possible network of nine species. Their existence in the solution is governed by four pK_a values of the sites of protonation or dissociation.

The pH, which affects the equilibrium concentrations of the various acid–base species, strongly influences cellular uptake or the binding of porphyrins to lipid membranes (3,8,11–13). As expected, a strong influence is observed from the protonation of the core nitrogens because the partitioning into the lipid environment of a charged tetrapyrrole ring is energetically not favorable. However, the ionization state of the peripheral carboxylic acids poses a more complex situation. Does the deprotonation of the carboxylates preclude the binding or the penetration of the charged porphyrin into the membrane? Or would the molecule be expected to reside in the membrane with its carboxylic ends located at the lipid–water interface, whether they are neutral or deprotonated, and so both forms could bind to a lipid membrane? In this case the extent of diminished binding of the anionic species could reflect the placement of the charged ends at the interface.

Determination of the pK_a values for dicarboxylic porphyrins in aqueous solutions is difficult because of pH-dependent aggregation phenomena. In addition, it is difficult to delineate, at any pH, the effect of protonation or deprotonation of the carboxylic moieties from the effect of protonation of the core nitrogen atoms. Therefore, we chose to study in this work the membrane-binding properties of two zinc (II) porphyrin complexes. Incorporation of Zn^{2+} ion into the porphyrin ring has two advantages. First, the protonation sites of the iminoporphyrin ring are blocked by the central ion, so they cannot interfere with carboxylic groups. There are thus only three possible ionic forms in aqueous solution. Second, metalloporphyrins tend less to form aggregates in aqueous solutions, probably because of the presence of water molecules as ligands to the core ion, which prevents stacked aggregates.

The subject of the present work is thus the acid–base properties of dicarboxylic metalloporphyrins, such as zinc-hematoporphyrin (ZnHP) and zinc-mesoporphyrin (ZnMP), whose chemical structures are shown in Fig. 1, and their interaction with liposomes, a simplified model for biological membranes (14). This study investigated the partitioning of the different ionic forms of the dyes into noncharged and negatively charged lipid vesicles at different pH values.

MATERIALS AND METHODS

Chemicals and sample preparation. ZnHP and ZnMP were purchased from Frontier Scientific, Inc. (Logan, UT). L-*a*-Phosphatidylcholine (PC, L-*a*-lecithin) type XIII-E from egg yolk (99%, solution of 100 mg/mL ethanol) was obtained from Sigma Chemical Co. (St. Louis, MO). It was a mixture of lipids with the following fatty acid makeup: 33% palmitic (C16:0), 31% oleic (C18:1), 13% stearic (C18:0) and 15% linoleic (C18:2). Other fatty acids are minor contributors to the fatty acid makeup (personal communication from Sigma). 1-Palmitoyl-2-oleoyl-*sn*-glycero-3-phosphate (POPA, >99%) was from Avanti Polar Lipids, Inc. (Alabaster, AL). This negatively charged lipid molecule has a composition that reflects most of the fatty acids in our PC. Triton X-100 (iso-octylphenoxypolyethanol

¶Posted on the web site on 16 September 2002.

*To whom correspondence should be addressed at: Department of Physics, Bar Ilan University, Ramat Gan 52900, Israel. Fax: 972-3-5353298; e-mail: ehren@mail.biu.ac.il.

†On leave from the Faculty of Chemistry, Jagiellonian University, 30-060 Kraków, Ingardena 3, Poland.

‡Incumbent of the Michael David Falk Chair in Laser Phototherapy.

Abbreviations: DMF, *N,N*-dimethylformamide; HP, hematoporphyrin IX; MCR, multivariate curve resolution; MP, mesoporphyrin IX; PC, L-*a*-phosphatidylcholine; PCA, principal component analysis; POPA, 1-palmitoyl-2-oleoyl-*sn*-glycero-3-phosphate; ZnHP zinc-hematoporphyrin IX; ZnMP, zinc-mesoporphyrin IX.

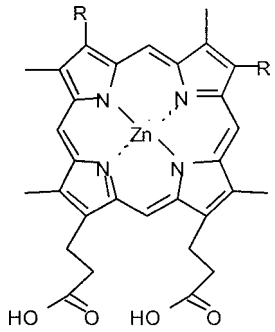

ZnHP: R= -CH(OH)CH_3

ZnMP: R= -CH_2CH_3

Figure 1. Chemical structures of the investigated metalloporphyrins.

containing approximately 10 molecules of ethylene oxide, scintillation grade) was obtained from BDH Chemicals Ltd. (Poole, UK). $Na_2HPO_4 \cdot 12H_2O$ was from Riedel-de Haën (Seelze, Germany). Citric acid and *N,N*-dimethylformamide (DMF) were obtained from Frutarom Ltd. (Haifa, Israel). Diethyl ether (>99.8%) was obtained from Fluka Chemie (Buchs, Switzerland).

For all subsequent work the dyes were dissolved in DMF forming a stock solution of nearly 1 m*M* concentration. In the final solutions the concentration of porphyrins was about 50 n*M*. All experiments were conducted in citrate–phosphate buffer. KCl was added up to a concentration of 0.15 *M* to keep the ionic strength constant.

Liposomes were prepared by sonication, as described previously (15). For mixed PC–POPA liposomes the stock solution of the lipid mixture (9:1 wt/wt) was prepared as follows: 0.9 mL ethanol solution of PC (90 mg) was poured into a vial, and the solvent was evaporated under nitrogen. Next, 1 mL of chloroform containing 10 mg of POPA was added to the vial. This was followed by hydration and sonication. For each pH value, a new stock solution of liposomes was prepared.

Measurements of K_b^{obs}. The kinetics of partitioning of the porphyrins to liposomes were studied for each case before the measurement of K_b, by using a fluorescence time-drive measurement, to determine the incubation time that was needed for full uptake equilibrium. A set of samples containing constant concentration of the dye with increasing concentrations of lipid was prepared. Emission spectra were recorded for the complete set after the incubation time.

Spectroscopic measurements. Absorption spectra were recorded on a Perkin–Elmer Lambda-9 UV–Vis–near-IR, computer-controlled spectrophotometer. Fluorescence excitation and emission spectra and fluorescence time-drive measurements were performed on a Perkin–Elmer digital fluorimeter (Model LS-50B, Norwalk, CT). All samples had low optical density (<0.05) at the wavelength of excitation to maintain a linear dependence of the fluorescence intensity on concentration.

Data treatment. All calculations were performed by using Matlab 6.1 software (The MathWorks, Inc., Natick, MA). For least squares nonlinear curve fitting we used the lsqcurvefit function from the Optimization Toolbox of Matlab 6.1. For principal component analysis (PCA) and multivariate curve resolution (MCR) (16) we used the commercial pca and mcr functions, respectively, from PLS_Toolbox ver. 2.1 (Eigenvector Research, Inc., Manson, OR). MCR was performed with the constraint that negative values of spectra and concentrations were not allowed.

Stability data. We determined the stability of the studied compounds in the dark, in the buffer solutions and when bound to liposomes. A set of *n* fluorescence spectra of ZnHP or ZnMP solutions, measured at various times after preparation, was organized in a ($n \times l$) matrix, where *l* is the number of spectral points in the fluorescence spectrum. Each of the spectra is a linear combination of *k* 'pure' component spectra with different weights (contributions to the total spectrum). The PCA method was used to determine the number of components (*k*) that constitute all the spectra in the set, with different weights in each spectrum. In case there was more than one component, MCR was applied to extract the pure component spectra and their concentration profiles.

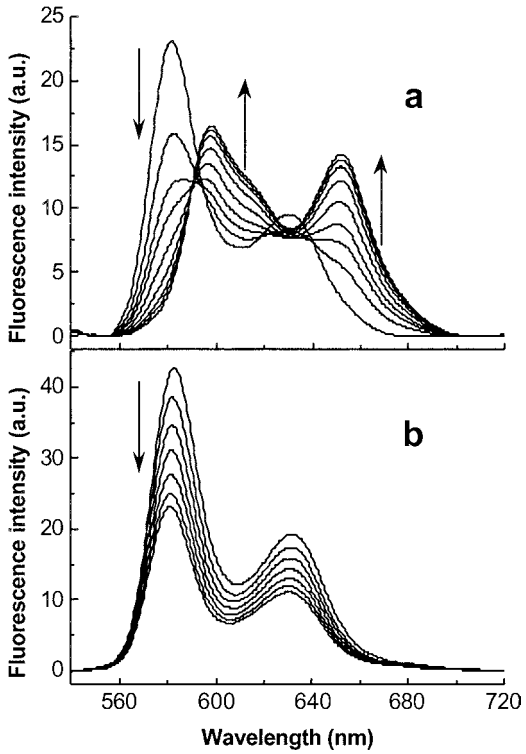

Figure 2. Change in fluorescence spectra of ZnHP (c = 46.4 n*M* in buffered solutions containing 0.15 *M* KCl; λ_{exc} = 404 nm) as a function of time: (a) pH 3.61, time: 0, 10, 20, 30, 50, 80, 120, 160, 210 min; and (b) pH 7.02, time: 0, 200, 400, 600, 800, 1000, 1160 min.

Determination of ionization constants. A set of fluorescence spectra of ZnHP solutions at constant concentration and different pH values was collected. For each pH at least four spectra were recorded immediately after preparation to avoid decomposition, and a final spectrum was obtained by averaging. Next, as above, the spectra were organized in a matrix, and PCA was carried out to decompose it into abstract factors (16). The reconstruction of the data matrix with three factors practically removed the experimental noise because it is secluded into separate factors during the decomposition. Again, MCR was performed on the reconstructed matrix to receive real pure component spectra and their concentration profiles.

RESULTS AND DISCUSSION

Stability of ZnHP and ZnMP

Although the stability of the metalloporphyrins is not the main interest of this study, it is a requirement for a correct determination of the acid dissociation and binding constants based on the fluorescence intensity. The stability of the porphyrins in the dark was studied in solutions having different pH in the absence and presence of liposomes by following the disappearance of the fluorescence as a function of time. The nature of the changes in the fluorescence spectra and their time course depended on the pH. The changes in emission spectra of ZnHP at pH 3.61 are presented in Fig. 2a. The fluorescence intensity at the emission maxima, at 582.5 and 630 nm, decreases with time, and two new bands, at 598 and 652 nm, arise. At pH 7.02 we observed only an overall decrease of the intensity of the whole spectrum (Fig. 2b). We applied the PCA method to determine the number of independent components that exist in the spectra (see Materials and Methods) and found two components for all stability measurements at pH lower than 6 and only one component for pH above 6. Figure 3a

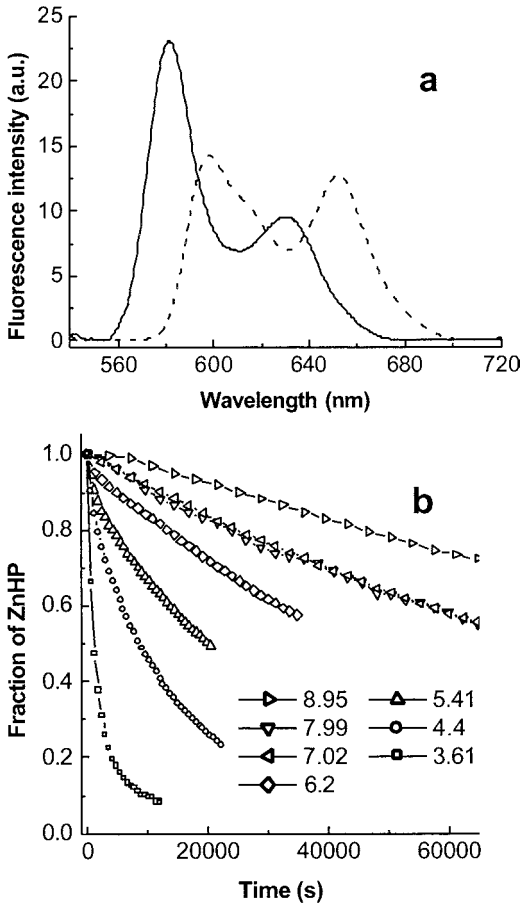

Figure 3. a: Fluorescence spectra of pure components received from multivariate curve resolution applied on the set of spectra depicted in Fig. 2a. Solid line is the spectrum of ZnHP, dashed line is the spectrum of the product. b: Concentration profiles of ZnHP during the decomposition process at different pH.

depicts the spectra of these pure components as obtained from MCR analysis applied to the spectra of ZnHP at pH 3.61 (Fig. 2a). The resolved spectrum of the product that is formed during the decomposition at the lower pH values (dashed line) is identical to that of pure HP at this pH (3,4,6,9). This behavior was also observed at pH 4.4 and 5.51. The concentration profiles of ZnHP at different pH as a function of time are shown in Fig. 3b.

The stability of ZnMP was checked in the same way. In this case we also observed the formation of metal-free MP for pH values below 6, whereas for pH $>$ 6 only a gradual loss in fluorescence intensity was observed, without the formation of new bands. Because ZnMP has an extremely low fluorescence for pH lower than 5 (see Fig. 4d), the experiment at pH 3.59 was conducted in a buffer–ethanol mixture (2:1 vol/vol).

In an acidified solution a metalloporphyrin can undergo demetallation according to the following equation (17):

$$ZnP + 2H^+ \rightleftharpoons Zn^{2+} + H_2P \quad (1)$$

Thus, at the initial stages of this reaction, the rate law for zinc removal should be first order in porphyrin. Of course, the free-base porphyrin that is formed will undergo subsequent processes, such as protonation of the iminonitrogens of the pyrrole ring or aggregation. Therefore, depending on the pH, both the monocation

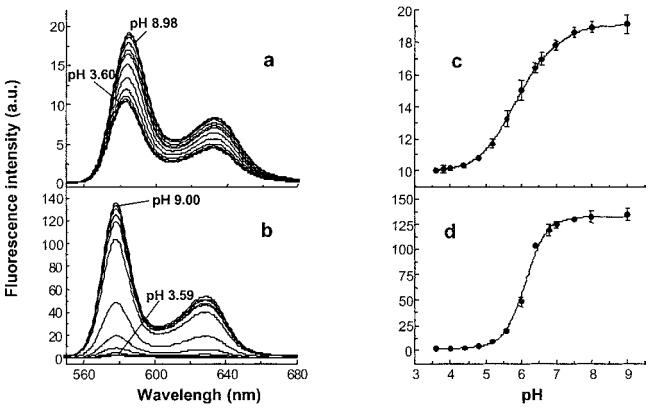

Figure 4. Fluorescence spectra of the investigated metalloporphyrins with increasing pH, in solutions containing 0.15 *M* KCl. a: ZnHP at concentration 46.4 n*M*, λ_{exc} = 408 nm, pH (from bottom to top) 3.6, 3.82, 4.0, 4.4, 4.8, 5.2, 5.61, 6.02, 6.41, 6.6, 6.99, 7.5, 8.0, 8.98. b: ZnMP at concentration 50.8 n*M*, λ_{exc} = 404 nm, pH (from bottom to top) 3.59, 4.0, 4.41, 4.8, 5.2, 5.59, 6.0, 6.4, 6.79, 7.0, 7.5, 7.98, 9. c: Fluorescence intensity of ZnHP (46.4 n*M*) *vs* pH; λ_{exc} = 408 nm, λ_{em} = 585 nm. d: Fluorescence intensity of ZnMP (50.8 n*M*) *vs* pH; λ_{exc} = 404 nm, λ_{em} = 578 nm.

(H_3P^+) and the dication (H_4P^{2+}) will exist, and these species will not tend to react again with zinc ions. The dimerization and aggregation phenomena are quite severe between pH 3 and 6 (4,6). We limited our consideration only to the initial stage of this complicated reaction. Under these conditions the concentration of H^+ is constant; thus, from the concentration profiles data we calculated the pseudo first-order rate constants of metalloporphyrin decomposition. The values are listed in Tables 1 and 2. The results of pseudo first-order kinetics at pH above 6, when demetallation is not observed, are also included in Tables 1 and 2.

The rate constants are strongly dependent on the pH of the surrounding medium. Incorporation of the dyes into lipid vesicles results in a considerable increase of the metalloporphyrin stability. Bárdos-Nagy *et al.* (18) determined the rate constants of Mg-mesoporphyrin (MgMP) decomposition to be 3.0×10^{-4} s^{-1} and 4.0×10^{-5} s^{-1} in phosphate buffer (pH 7.4, 32°C) and in suspension of 1,2-dimyristoyl-*sn*-glycero-3-phosphatidylcholine/1,2-dimyristoyl-*sn*-glycero-3-phosphatidylglycerol liposomes (19:1 wt/wt) in phosphate buffer (pH 7.4, 32°C), respectively. The decomposition rate constants that we report in this study for ZnMP are lower than the above values. This should be expected based on the classification of Zn-metalloporphyrius in the more resistant stability class III, as compared with the less stable class IV of the Mg complexes (19).

pKa values of ZnHP and ZnMP

Figure 4a,b presents fluorescence spectra recorded upon acid–base titration of ZnHP and ZnMP solutions, respectively. Figure 4c,d shows the pH dependence of the intensity at the fluorescence maximum. In the case of ZnHP, lowering the pH leads to a decrease of the fluorescence emission intensity and to a gradual hypsochromic shift of the maximum from 585 to 582.5 nm. Acidification of the ZnMP solution, in the same pH range, resulted in a more drastic decrease of the fluorescence intensity, but with a concomitant negligible (less than 1 nm) shift of the peak's location. For both cases the loss in intensity of emission upon lowering the pH can be attributed to the formation of nonfluorescent aggregates (20,21).

Table 1. Rate constants of ZnHP decomposition in different systems

System	Number of components	Rate constant (s^{-1})
Buffer pH 3.61	2	$(6.91 \pm 0.34) \times 10^{-4}$
Buffer pH 4.40	2	$(2.09 \pm 0.19) \times 10^{-4}$
Buffer pH 5.41	2	$(6.67 \pm 0.53) \times 10^{-5}$
Buffer pH 6.20	1	$(1.52 \pm 0.02) \times 10^{-5}$
Buffer pH 7.02	1	$(9.13 \pm 0.31) \times 10^{-6}$
Buffer pH 7.99	1	$(8.9 \pm 0.1) \times 10^{-6}$
Buffer pH 8.95	1	$(6.1 \pm 0.2) \times 10^{-6}$
Liposomes in buffer pH 3.61	1	$(1.93 \pm 0.03) \times 10^{-5}$
Liposomes in buffer pH 8.99	1	$(1.01 \pm 0.02) \times 10^{-6}$

Table 2. Rate constants of ZnMP decomposition in different systems

System	Number of components	Rate constant (s^{-1})
Buffer + ethanol (2:1 vol/vol) pH 3.60	2	$(8.71 \pm 0.41) \times 10^{-4}$
Buffer pH 5.40	2	$(8.15 \pm 0.52) \times 10^{-4}$
Buffer pH 6.19	1	$(2.05 \pm 0.18) \times 10^{-4}$
Buffer pH 7.00	1	$(1.69 \pm 0.45) \times 10^{-4}$
Buffer pH 7.99	1	$(6.75 \pm 1.55) \times 10^{-5}$
Buffer pH 8.99	1	$(2.62 \pm 0.67) \times 10^{-5}$
Liposomes in buffer pH 4.40	1	$(4.91 \pm 0.02) \times 10^{-6}$

Porphyrins are known to aggregate readily in aqueous surroundings. Dimerization constants for free-base porphyrins were measured in aqueous solution, at 25°C and pH 7.2, to be $4.0 \times 10^5\ M^{-1}$ for HP (22) and $5.4 \times 10^6\ M^{-1}$ for MP (23). One would expect the extent of dimerization to vary from one ionic form to another and also to increase at lower pH (dimerization or aggregation is favored when the carboxylic chains are uncharged), but the constants mentioned above clearly show the higher tendency of the less polar MP to aggregate in water. One can expect the same trends for the zinc complexes.

To prevent the dimerization and aggregation processes, surfactants are usually added to form micelles. We repeated the acid–base titration experiments of the dyes in solutions containing 0.6% of Triton X-100. For ZnMP the shape and intensity of emission spectra were not dependent on pH, and for ZnHP we observed only small changes in both features. This is probably a result of the fact that the chromophoric part of the molecules is inside the nonpolar micellar environment and is only slightly affected by the protonation state of the carboxylates. This effect of micelles confirms the occurrence of aggregation processes in the aqueous solutions of the investigated metalloporphyrins.

The change in the band's maximum location of ZnHP is a result of the acid–base equilibrium. One would not expect, *a priori*, a significant influence of the ionization state of the propionic acid groups on the spectroscopic properties of the porphyrins' pyrrole system, to which they are not coupled electronically. We indeed observed only a small shift in the case of ZnHP and almost no shift for ZnMP. According to Brault (13) the fluorescence properties of the porphyrin might be affected by the solvation, which is expected to depend on the protonation state of carboxyl chains.

Recently, some work was done on PCA and deconvolution of heavily overlapped spectra (24–26). We used the statistical data processing methods of PCA and then MCR to resolve the spectra presented in Fig. 4a. Assuming the constraints that the spectra at pH 8.95 and 3.61 are pure spectra of the dianionic and the neutral forms of ZnHP, respectively, enabled us to deconvolve the spectrum of the monoanionic species and the concentration profiles of these three forms (shown in Fig. 5). Scheme 1 shows the equlibria that exist in an aqueous solution of ZnHP. pK_{a2} was obtained by fitting a sigmoidal curve to the concentration profile of the dianion species in Fig. 5. The fitted line is shown in the figure; the value of pK_{a2} was 6.9 ± 0.05. Fitting a sigmoidal curve to the concentration profile of the neutral species in Fig. 5 yields a pK_{a1} of 5.7 ± 0.1. The fitted line is also shown in the figure.

The ionization constants of the two propionic acid groups in free-base porphyrins were determined earlier. Brault *et al.* (3) reported the values of 5.0 and 5.4 for HP and 5.4 and 6.0 for deuteroporphyrin, using a fluorescence method. Barret *et al.* (5) performed volumetric titrations of aqueous solutions of HP and obtained different results, depending on the starting solution. The pK_a values that were obtained by basic titration from an acidic medium were 6.0 ± 0.1 and 6.8 ± 0.1 and were different from those obtained by acid titration from an alkaline medium: 5.75 ± 0.1 and 6.5 ± 0.1. Our results for ZnHP are in good agreement with those for HP from the volumetric experiments.

Interaction of ZnHP and ZnMP with liposomes

The partitioning of the tested compounds between the bulk aqueous phase and lipid vesicles was examined as a function of pH in the range 3.6–9. For each pH a set of emission spectra was recorded while the lipid concentration was varied from 0 to 0.57 mg/mL. The following formula (27–29) was used to evaluate an effective binding constant, K_b^{obs}, which is a weighted average of the binding constants of various species (see Eq. 8 and the discussion thereof):

$$F = \frac{F_{init} + F_{comp} K_b^{obs}[L]}{1 + K_b^{obs}[L]} \quad (2)$$

where F_{init}, F and F_{comp} are, respectively, the fluorescence intensities of the dye that is measured in solutions before adding any lipid, with lipid at concentration [L] and that is obtained asymptotically at complete binding. To obtain the K_b for each compound, F *vs* [L] data were plotted and fitted to Eq. 2 by a nonlinear regression routine. The calculated binding constants are listed in Table 3. Figure 6 depicts the correlations between the measured K_b^{obs} and the pH. For both metalloporphyrins we observed a strong dependence of the partitioning to the lipid phase on the acidity of the bathing solution. The reduction of the K_b^{obs} values with increasing pH from 5.4 to 9.0 is more pronounced for ZnHP (a 3.9-fold factor) than for ZnMP (2.5 times) in the presence of neutral liposomes.

The instability and aggregations processes, which are more significant at lower pH, are the reason for the higher inaccuracy of the measured binding constants at low pH, which is reflected by the error bars upon reduction of pH (see Fig. 6) The phenomena mentioned above became a serious problem in the measurements with ZnMP at pH 4.4. At lower pH values we were not able to obtain any reasonable results.

Surface charge can be an important factor in the interaction of charged molecules with liposomes. The surface of most biomembranes is negatively charged due to the presence of acidic

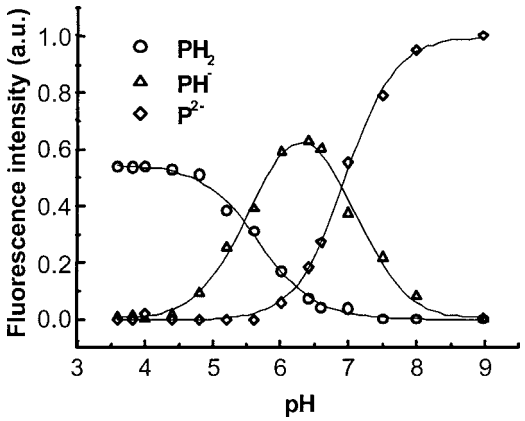

Figure 5. Fluorescence intensity variation of each species of ZnHP in buffer as a function of pH.

phospholipids. Typically, 10–20% of the membrane lipids are anionic (30). We used neutral (PC) and negatively charged (PC–POPA, 9:1 wt/wt) lipids (pK_a of the phosphate is approximately 1–2) in the binding studies of ZnMP. Existence of the negative charges on the surface of PC–POPA liposomes resulted in a bigger reduction of the binding constants (a 5.5-fold factor) with increasing pH values as compared with neutral liposomes, as seen in Table 3 and in Fig. 6 (closed circles).

Galántai *et al*. (31) investigated the partitioning of free-base MP to neutral membranes (1,2-dimyristoyl-*sn*-glycero-3-phosphatidylcholine) and to a negatively charged one (1,2-dimyristoyl-*sn*-glycero-3-phosphatidylcholine/1,2-dimyristoyl-*sn*-glycero-3-phosphatidylglycerol, 19:1 wt/wt) at pH 7.4 and 32°C. They found the values of binding constants to be 190 ± 45 and 47 ± 9 $(mg/mL)^{-1}$, respectively, demonstrating the effect of charges on lowering the binding constant of the ionized MP. Bárdos-Nagy *et al*. (18) found the binding constant of MgMP to charged liposomes composed of 1,2-dimyristoyl-*sn*-glycero-3-phosphatidylcholine/1,2-dimyristoyl-*sn*-glycero-3-phosphatidylglycerol (19:1 wt/wt) at pH 7.4 and 32°C to be equal to 22 $(mg/mL)^{-1}$. This value is comparable to that of ZnMP in the PC–POPA liposomes found in the present study.

The dependence of the effective overall binding constant, K_b^{obs} on pH, as seen in Fig. 6, can be explained by the different affinities of the various protonated forms of the dye for the lipid bilayer, each thus having a different binding constant. Scheme 1 summarizes the processes occurring in an aqueous solution of a dipropionic metalloporphyrin, which also contains lipid vesicles.

The effective binding constant, K_b^{obs}, can be defined as

$$K_b^{obs} = \frac{c_L}{c_w[L]} \tag{3}$$

where c_L and c_w are the total concentrations of the metalloporphyrin in the lipid and water phases, respectively. Assuming that all ionic species can partition into the lipid phase,

$$c_L = [PH_2 - L] + [PH^- - L] + [P^{2-} - L] \tag{4}$$

where $[PH_2 - L]$, $[PH^- - L]$ and $[P^{2-} - L]$ represent the concentrations of the membrane-incorporated neutral, monoanionic and dianionic forms of the metalloporphyrin, respectively. The total concentration of all the species in the aqueous phase is

$$c_w = [PH_2] + [PH^-] + [P^{2-}] \tag{5}$$

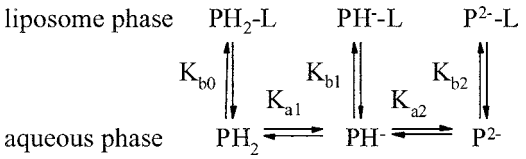

Scheme 1.

The dissociation constants are defined as

$$K_{a1} = \frac{[PH^-][H^+]}{[PH_2]}, \qquad K_{a2} = \frac{[P^{2-}][H^+]}{[PH^-]}, \tag{6}$$

The binding constants of the various metalloporphyrin forms to the liposomes are defined by

$$K_{b0} = \frac{[PH_2 - L]}{[PH_2][L]}, \qquad K_{b1} = \frac{[PH^- - L]}{[PH^-][L]},$$
$$K_{b2} = \frac{[P^{2-} - L]}{[P^{2-}][L]} \tag{7}$$

By simple mathematical operations we obtain the following expression for K_b^{obs}:

$$K_b^{obs} = K_{b0}\frac{1}{\alpha} + K_{b1}\frac{1}{\beta} + K_{b2}\frac{1}{\gamma} \tag{8}$$

where

$$\alpha = 1 + 10^{(pH - pK_{a1})} + 10^{(2pH - pK_{a1} - pK_{a2})} \tag{9}$$
$$\beta = 1 + 10^{(pK_{a1} - pH)} + 10^{(pH - pK_{a2})} \tag{10}$$
$$\gamma = 1 + 10^{(pK_{a2} - pH)} + 10^{(pK_{a1} + pK_{a2} - 2pH)} \tag{11}$$

From Eqs. 8–11 it follows that five parameters (pK_{ai} and K_{bi} values) need to be determined, but for some of them we can make reasonable assumptions.

Assuming that K_{b0} and K_{b2} are identical to K_b^{obs} under the extreme conditions of pH 3.61 and 8.95, respectively, we fitted our results for ZnHP to Eq. 8. The best fit, which is shown in Fig. 6a as a full line, was obtained with the binding and ionization constant values reported in Table 4. In the case of ZnMP in the suspension of PC liposomes in buffer, the results did not allow us to make any assumption about K_{b0} because of the instability and aggregation processes at low pH. Therefore, we assumed K_b^{obs} for pH 8.99 to be equal to K_{b2}, and the same value of pK_{a2} as was found for ZnHP. In the case of ZnMP in the presence of PC–POPA liposomes, we assumed the same values of both ionization constants as for the

Table 3. Experimentally measured binding constants (K_b^{obs})

ZnHP in PC liposomes		ZnMP in PC liposomes		ZnMP in PC–POPA liposomes	
pH	K_b^{obs} $(mg/mL)^{-1}$	pH	K_b^{obs} $(mg/mL)^{-1}$	pH	K_b^{obs} $(mg/mL)^{-1}$
3.61	49.9 ± 7.6	4.40	152.8 ± 18.2		
4.40	47.2 ± 9.1	5.00	159.7 ± 12.6		
5.41	38.0 ± 5.7	5.40	152.4 ± 5.1	5.40	138.4 ± 15.2
6.20	24.1 ± 4.4	6.19	108.7 ± 5.2	6.20	77.3 ± 8.1
7.00	16.2 ± 3.5	7.00	82.2 ± 7.5	7.00	46.7 ± 7.4
7.99	11.0 ± 2.5	7.99	61.8 ± 6.1	8.00	33.8 ± 4.4
8.95	9.72 ± 2.01	8.99	59.85 ± 3.2	8.96	25.2 ± 5.4

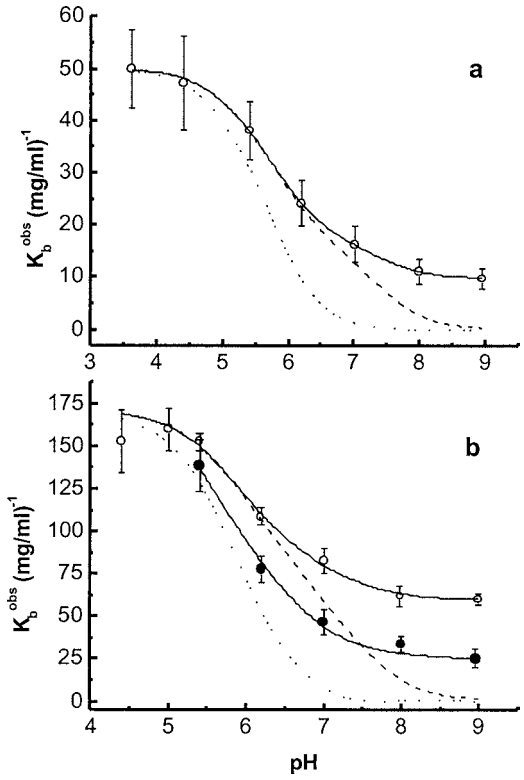

Figure 6. Dependence of K_b^{obs} on the pH: (a) ZnHP, (b) ZnMP, (○) for PC liposomes, (●) for PC–POPA liposomes. Solid lines correspond to the fitting of the results to Eq. 8. Dotted and dashed lines show the hypothetical dependence when only neutral forms or neutral and monoanionic forms bind to the liposomes, respectively.

neutral liposomes and found K_{b2} to be identical to K_b^{obs} measured at the pH 8.96. The fitted parameters for ZnMP are listed in Table 4.

Equation 8 enables the consideration of membrane partitioning of all three porphyrin species, each with its characteristic binding constant, as was described in the previous paragraph. If, however, the dianionic porphyrin does not partition into the membrane, K_{b2} has to be taken as 0, and the results of the calculations based on Eq. 8 are the dashed lines in Fig. 6. If only the neutral porphyrin partitions, both K_{b1} and K_{b2} equal 0, and the calculation yields the dotted lines. It can be seen clearly that both the dashed and the dotted lines do not fit to the experimental points; thus, both assumptions are wrong, and it appears that all three porphyrin species are capable of partitioning into the membrane.

The salient findings that are deduced from Table 4 are that (1) all forms of the more hydrophobic ZnMP bind much stronger than the corresponding ZnHP species; (2) the effect of deprotonation in impeding the partitioning into the membrane is stronger for ZnHP than for ZnMP. The reasoning could be that increasing the polarity of a molecule that is already more hydrophyllic has a stronger effect than increasing the polarity of a more hydrophobic molecule. Yet even the charged, deprotonated forms partition into the liposomes, and (3) a negative surface charge lowers the binding of the dianionic ZnMP more than the binding of the monoanionic species and has practically no effect on the neutral species.

The pK_a values obtained for the systems with liposomes are slightly higher than those we measured for ZnHP in water and those found in the literature (3,5) and could be compared with those determined in the presence of surfactant micelles or other

Table 4. Values of ionization and binding constants

System	pK_{a1}	pK_{a2}	K_{b0} $(mg/mL)^{-1}$	K_{b1} $(mg/mL)^{-1}$	K_{b2} $(mg/mL)^{-1}$
ZnHP in PC liposomes	5.62	7.24	49.9	18.7	9.72
ZnMP in PC liposomes	5.88	7.24	171.5	84.7	59.85
ZnMP in PC–POPA liposomes	5.88	7.24	167.5	45.8	25.2

liposomes. A similar observation of the effect of the chromophore's environment on the pH was reported by Barrett *et al.* (5), who found pK_a of 6.5 ± 0.1 and 7.2 ± 0.1 for HP solubilized on sodium dodecyl sulfate micelles. Kuzelová and Brault (32) and Maman and Brault (33) investigated the interactions of deuteroporphyrin with PC vesicles. They found, in the presence of dimyristoylphosphatidylcholine, pK_a of 6.5 ± 0.3 and 7.2 ± 0.2.

When charged phospholipids are included, the liposomes carry a surface charge and surface (Gouy–Chapman) potential (34). Assuming a surface area of 60 $Å^2$ per molecule (30), the charge density in our PC–POPA liposomes is approximately 1:600 electron charges/$Å^2$. Under our experimental conditions of 0.15 *M* concentration of electrolyte, we calculated the surface potential to be −28.4 mV (34). This negative potential is a force that tends to lower the binding or partitioning capacity of negatively charged molecules. This is clearly seen in Fig. 6 and Table 4.

In summary, using metalloporphyrins enabled us to isolate the effect of the ionic status of the carboxylates on the membrane-binding properties. We were able to evaluate the pK_a of the two carboxylic acids of ZnHP in buffer and also the pK_a of ZnHP and ZnMP in the presence of liposomes. We found that all three species of each porphyrin do partition into the membrane, even the dianionic molecule. We were able to extract the binding constants of all these species and found indeed that increasing the charge on the porphyrin lowers the binding constant. In addition, generating a surface charge on the membrane also causes a gradual reduction in the binding constant, depending on the charge of the molecule. These findings suggest that the porphyrin is located in the membrane with its carboxylic ends near the interface. Additional proof of this was given recently in a study of the effect of the vertical location of a porphyrin in a membrane on its sensitizing efficiency (27).

Acknowledgements—We acknowledge the support (Grant 9800364) of the United States–Israel Binational Science Foundation (BSF), Jerusalem, Israel. We also acknowledge the support of the Michael David Falk Chair in Laser Phototherapy.

REFERENCES

1. Srivastava, R. C., V. D. Anand and W. R. Carper (1973) A fluorescence study of hematoporphyrin. *Appl. Spectrosc.* **27**, 444–449.
2. Savitski, A. P., E. V. Vorobyora, I. V. Berezin and N. N. Ugarova (1981) Acid-base properties of protoporphyrin IX; its dimethyl ester and heme solubilized on surfactant micelles: spectrophotometric and fluorimetric titration. *J. Colloid Interface Sci.* **84**, 175–181.
3. Brault, D., C. Vever-Bizet and T. Le Doan (1986) Spectrofluorimetric study of porphyrin incorporation into membrane models—evidence for pH effects. *Biochim. Biophys. Acta* **857**, 238–250.
4. Pottier, R. H., J. C. Kennedy, Y. F. A. Chow and F. Cheung (1988) The pKa values of hematoporphyrin IX as determined by absorbance and fluorescence spectroscopy. *Can. J. Spectrosc.* **33**, 57–62.

5. Barrett, A. J., J. C. Kennedy, R. A. Jones, P. Nadeau and R. H. Pottier (1990) The effect of tissue and cellular pH on the selective biodistribution of porphyrin-type photochemotherapeutic agents: a volumetric titration study. *J. Photochem. Photobiol. B: Biol.* **6**, 309–323.
6. Chapados, C., D. Girard, M. Trudel and M. Ringuet (1995) Separation of overlapping spectra from evolving systems using factor-analysis. 4. Fluorescence-spectra of hematoporphyrin-IX. *Biophys. Chem.* **55**, 289–300.
7. Chapados, C., D. Girard, M. Trudel and M. Ringuet (1995) Separation of overlapping spectra from evolving systems using factor-analysis. 3. Fluorescence-spectra of hematoporphyrin-IX di-*n*-propylether diethanolamide. *Biophys. Chem.* **54**, 165–174.
8. Cunderlíková, B., L. Gangeskar and J. Moan (1999) Acid-base properties of chlorin e6: relation to cellular uptake. *J. Photochem. Photobiol. B: Biol.* **53**, 81–90.
9. Cunderlíková, B., E. G. Bjørklund, E. O. Pettersen and J. Moan (2001) pH dependent spectral properties of HP IX, TPPS2a, mTHPP and mTHPC. *Photochem. Photobiol.* **74**, 246–252.
10. Brault, D. and C. Vever-Bizet (1992) Protonation equilibria of hematoporphyrin as studied by fluorescence lifetime analysis. *J. Chem. Soc. Faraday Trans.* **88**, 1519–1524.
11. Brault, D., C. Vever-Bizet and K. Kuzelova (1993) Interactions of dicarboxylic porphyrins with membranes in relation to their ionization state. *J. Photochem. Photobiol. B: Biol.* **20**, 191–195.
12. Kuzelova, K. and D. Brault (1995) Interactions of dicarboxylic porphyrins with unilamellar lipidic vesicles—drastic effects of pH and cholesterol on kinetics. *Biochemistry* **34**, 11245–11255.
13. Brault, D. (1990) Physical chemistry of porphyrins and their interactions with membranes: the importance of pH. *J. Photochem. Photobiol. B: Biol.* **6**, 79–86.
14. Hoebeke, M. (1995) The importance of liposomes as models and tools in the understanding of photosensitization mechanisms. *J. Photochem. Photobiol. B: Biol.* **28**, 189–196.
15. Kepczynski, M., R. P. Pandian, K. M. Smith and B. Ehrenberg (2002) Do liposome-binding constants of porphyrins correlate with their measured and predicted partitioning between octanol and water? *Photochem. Photobiol.* **76**, 127–134.
16. Malinowski, E. R. (1991) *Factor Analysis in Chemistry*. Wiley-Interscience Publication, New York.
17. Phillips, J. N. (1960) The ionization and coordination behaviour of porphyrins. *Rev. Pure Appl. Chem.* **10**, 35–60.
18. Bárdos-Nagy, I., R. Galántai, A. D. Kaposi and J. Fidy (1998) Difference in the transport of metal and free-base porphyrins. Steady-state and time-resolved fluorescence studies. *Int. J. Pharm.* **175**, 255–267.
19. Buchler, J. W. (1975) Static coordination chemistry of metalloporphyrins. In *Porphyrins and Metalloporphyrins*, (Edited by K. M. Smith), pp. 157–231. Elsevier Scientific Publishing Company, Amsterdam.
20. Pottier, R. and T. G. Truscott (1986) The photochemistry of hematoporphyrin and related systems. *Int. J. Radiat. Biol.* **50**, 421–452.
21. Hambright, P. (1975) Dynamic coordination chemistry of metalloporphyrins. In *Porphyrins and Metalloporphyrins*, (Edited by K. M. Smith), p. 265. Elsevier Scientific Publishing Company, Amsterdam.
22. Margalit, R., N. Shaklai and S. Cohen (1983) Fluorimeteic studies on the dimerization equlibrium of protoporphyrin IX and its haemato derivative. *Biochem. J.* **209**, 547–552.
23. Margalit, R. and M. Rotenberg (1984) Thermodynamics of porphyrin dimerization in aqueous solutions. *Biochem. J.* **219**, 445–450.
24. Šašic, S. (2001) Eigenvalues and principal component loadings of heavily overlapped vibrational spectra. *Spectrochim. Acta, A* **57**, 323–336.
25. Shen, C., T. J. Vickers and C. K. Mann (1992) Abscissa error-detection and correction in Raman-spectroscopy. *Appl. Spectrosc.* **46**, 772–777.
26. Shen, C., A. J. Peacock, R. G. Alamo, T. J. Vickers, L. Mandelkern and C. K. Mann (1992) Structural studies of crystalline linear polyethylenes as revealed by factor-analysis of their Raman-spectra. *Appl. Spectrosc.* **46**, 1226–1230.
27. Lavi, A., H. Weitman, R. T. Holmes, K. M. Smith and B. Ehrenberg (2002) The depth of a porphyrin in a membrane and the membrane's physical properties strongly affect the photosensitizing efficiency. *Biophys. J.* **82**, 2101–2110.
28. Ehrenberg, B. (1992) Assessment of the partitioning of probes to membranes by spectroscopic titration. *J. Photochem. Photobiol. B: Biol.* **14**, 383–386.
29. Roslaniec, M., H. Weitman, D. Freeman, Y. Mazur and B. Ehrenberg (2000) Liposome binding constants and singlet oxygen quantum yields of hypericin, tetrahydroxy helianthrone and their derivatives: studies in organic solutions and in liposomes. *J. Photochem. Photobiol. B: Biol.* **57**, 149–158.
30. Gennis, R. B. (1989) *Biomembranes—Molecular Structure and Function*. Springer Verlag, New York.
31. Galántai, R., I. Bárdos-Nagy, K. Módos, J. Kardos, P. Závodszky and J. Fidy (2000) Serum albumin-lipid membrane interaction influencing the uptake of porphyrins. *Arch. Biochem. Biophys.* **373**, 261–270.
32. Kuzelová, K. and D. Brault (1995) Interactions of dicarboxylic porphyrins with unilamellar lipidic vesicles: drastic effect of pH and cholesterol on kinetics. *Biochemistry* **34**, 11245–11255.
33. Maman, N. and D. Brault. (1998) Kinetics of the interactions of a dicarboxylic porphyrin with unilamellar lipidic vesicles: interplay between bilayer thickness and pH in rate control. *Biochim. Biophys. Acta* **1414**, 31–42.
34. McLaughlin, S. (1977) Electrostatic potentials at membrane-solution interfaces. *Curr. Top. Membr. Transp.* **9**, 71–144.